Particle motion near the resonant surface of a high-frequency wave in a magnetized plasma

J. J. Martinell
Instituto de Ciencias Nucleares,
Universidad Nacional Autónoma de México
A. Postal 70-543, 04510 México D.F.
e-mail: martinel@nuclecu.unam.mx

Recibido el 11 de enero de 2002; aceptado el 4 de febrero de 2002

The motion of single charged particles in a magnetized plasma is studied using a Lagrangian formalism, applied to the average over a gyroperiod, in the presence of an electromagnetic wave that is being resonantly absorbed by the medium. Near the resonance surface the wave amplitude has a gradient and the resulting particle drifts are shown to be consistent with the existence of a ponderomotive force, produced by the wave-field-gradient. The orbits are also obtained numerically to show how the drifting motion arises, and to study the case of high field-gradients, which is not described with the formal analysis.

Keywords: Charged particle orbits; electromagnetic waves in plasmas; lagrangian mechanics.

Se estudia el movimiento de partículas cargadas individuales en un plasma magnetizado con un formalismo Lagrangiano, aplicado al promedio sobre un período de giro, en presencia de una onda electromagnética que es absorbida de manera resonante por el medio. Cerca de la superficie de resonancia la amplitud de la onda tiene un gradiente y se muestra que los movimientos de deriva resultantes son consistentes con la existencia de una fuerza ponderomotriz, producida por el gradiente del campo de la onda. También se obtienen las órbitas numéricamente para mostrar cómo es el movimiento de deriva y para estudiar el caso de gradientes de campo grandes, que no se describe adecuadamente con el análisis formal.

Descriptores: Orbitas de partículas cargadas; ondas electromagnéticas en plasmas; mecánica lagrangiana.

PACS: 52.20.Dq; 52.35.Hr; 45.20.Jj

1. Introduction

The use of electromagnetic waves to heat a plasma has been studied for many years in relation to magnetic confinement fusion applications. It is now clear that for a plasma to reach the required high temperatures for nuclear fusion to be sustained, it will be necessary to inject energy in the form of radio frequency (rf) waves or energetic neutral beams. The wave is absorbed at the resonance frequency of the charged particles (electrons or ions) gyrating in the magnetic field, which occurs at a specific location in the plasma, since the magnetic field varies with position. At this resonant surface, the wave amplitude decreases and therefore, in front of the surface, the wave fields have a gradient in the direction of wave propagation. It is known that an oscillating field with a spatial variation produces a time-averaged ponderomotive (PM) force in the direction opposite to the field gradient, so one would expect to have such a force in the vicinity of the resonant surface. The momentum transfered to the plasma by a PM force has been invoked as the cause of the rotation produced in toroidal experiments, when the injected rf wave is not resonant [1]. But also, for resonant absorption of high-frequency rf waves it is possible to have a rotation due to the PM force, as proposed in Ref. 2. These waves resonate with electron cyclotron (EC) frequency and their absorption is in a very localized region of the plasma, which may give rise to quite high field gradients.

The physical origin of the PM force is quite clear, when one considers an unmagnetized plasma in presence of a rf wave. Essentially, a field gradient parallel to the field itself, gives an oscillating particle a larger push in one direction than in the other, which produces the effect of a net force along the negative field gradient, when averaged over a wave period. The physics is less clear when there is a background magnetic field, since there are two frequencies involved, and the gradient does not necessarily have to be parallel to the wave field. If the magnetic field is weak enough, such that the wave frequency ω is larger than the cyclotron frequency Ω, as the particles gyrate they feel the effect of the wave fields averaged over the wave oscillations, and experience a drifting motion of their guiding center; one would expect the drift to be the result of the PM force crossed with the magnetic field. However, when Ω is of the order of, or larger than ω, the averaging procedure over the wave period, interferes with the gyromotion and the concept of ponderomotive force becomes confused.

In this paper we look at the particle motion in the combined fields of a rf wave and a background magnetic field, $\mathbf{B}_0$, under different circumstances, relevant to the problem of rf heating of a toroidal magnetized plasma, in order to elucidate the effect of the wave gradients on the particle fluxes. Of particular importance to us is the use of electron cyclotron waves to produce a particle flux in the vicinity of the resonant surface. The situation we consider is that, an EC wave propagating in the radial direction (perpendicular to the mag-

netic field) arrives at the resonant surface, where it is mostly absorbed and thus its amplitude has a radial gradient; the particle (electron or ion) motion in these fields is then studied, including the case of large wave amplitude, [2] and for ω equals to any harmonic of Ω. The two wave polarizations, the ordinary (O-mode), with the wave E-field parallel to $\mathbf{B}_0$, and extraordinary (X-mode), with the wave E-field perpendicular to $\mathbf{B}_0$, are considered. We first adopt a Lagrangian description of the particle orbits, using averages over the gyromotion. This is done in Sec. 2 where we obtain the drift velocity of the guiding center, and it is identified as produced by a ponderomotive force. Then, in Sec. 3 the equations of motion are numerically solved to display the orbits directly and show how the drifting motion is actually occurring. In this way it is also possible to consider extreme cases that are not possible to describe with an analytical description. It is shown that, in most resonant cases, the drifting motion of the guiding center is not accompanied by a matching particle orbit displacement, as in the $\mathbf{E}\times\mathbf{B}$ drift, for instance, but rather the increasing radius causes the guiding center displacement. This does produce an average particle flux, but it is limited by the geometrical size of the device and the gradient scale lengths. Finally, in Sec. 4 we comment on the application of our results and give the conclusions.

2. Lagrangian particle motion

In order to analyze the motion of a charge particle in a magnetic field, and influenced by the action of an electromagnetic field, we follow a Lagrangian description. Since the background magnetic field is assumed to be larger than the wave field, the gyromotion of the particle in the strong field is dominant and it is then possible to consider the wave as a perturbation. Thus, the Lagrangian is averaged over a gyroperiod, so that, the Euler-Lagrange equations resulting from the variational principle for the averaged Lagrangian, give the motion of the guiding center. The Lagrangian than we will use is a phase space Lagrangian that is a function of the coordinates $\mathbf{q}$, velocities $\dot{\mathbf{q}}$ and the momentum $\mathbf{p}$, obtained from a Hamiltonian $H(\mathbf{p},\mathbf{q},t)$ as [4]

$$L(\mathbf{q},\mathbf{p},\dot{\mathbf{q}},t)=\mathbf{p}\cdot\dot{\mathbf{q}}-H(\mathbf{q},\mathbf{p},t), \tag{1}$$

where the relativistic H for a particle in an electromagnetic field is given by

$$H(\mathbf{q},\mathbf{p},t)=[m^2c^4+c^2(\mathbf{p}-q/c\mathbf{A})^2]^{1/2}+q\phi.$$

The fields are given in terms of the electromagnetic potentials ϕ and $\mathbf{A}$, while the canonical momentum is

$$\mathbf{p}=m\gamma\mathbf{v}+q/c\mathbf{A},$$

where γ is the relativistic factor. In this description, the velocities $\dot{\mathbf{q}}$, and momenta $m\gamma\mathbf{v}$, are treated as independent variables, although there is a relation among them, which will come as a result of the Euler-Lagrange equations. It is actually more convenient to work with a variable $\mathbf{u}=\gamma\mathbf{v}$, instead of the velocity or the momentum.

For a uniform B field in the z-direction, the relevant vector potential is, $\mathbf{A}=B_0x\hat{y}$. For simplicity we adopt cartesian coordinates, which are valid locally. To represent O- and X-modes we use the following potentials:

$$\mathbf{A}_o=B_0x\hat{y}+\int B_1(x)\cos(kx-\omega t)dx\hat{z}, \tag{2}$$

$$\mathbf{A}_x=[B_0x+A_2(x)\sin(kx-\omega t)]\hat{y} -A_1(x)\cos(kx-\omega t)\hat{x}, \tag{3}$$

and choose a gauge where $\phi=0$. For the X-mode a longitudinal component is included, according to the characteristic elliptic polarization of this mode. The amplitudes are functions of x, the wave propagation direction. For definiteness, here we will take an exponential dependence, $B_1(x)=B_1\exp(-ax)$ and the same for A_1 and A_2. Note that in order to have a spatially dependent amplitude it is necessary to have field sources present; a plane wave in vacuum is homogeneous. However, we do not consider the effect of the plasma on the wave here. With this variation, the corresponding wave fields are,

$$\mathbf{E}_{1o}=\frac{\omega}{c}\frac{B_1\exp(-ax)}{k^2+a^2}[k\cos(kx-\omega t) +a\sin(kx-\omega t)]\hat{z}, \tag{4}$$

$$\mathbf{B}_{1o}=-B_1\exp(-ax)\cos(kx-\omega t)\hat{y}, \tag{5}$$

$$\mathbf{E}_{1x}=\frac{\omega}{c}\exp(-ax)[A_1\cos(kx-\omega t)\hat{y} +A_2\sin(kx-\omega t)\hat{x}], \tag{6}$$

and

$$\mathbf{B}_{1x}=A_1\exp(-ax)[k\cos(kx-\omega t) -a\sin(kx-\omega t)]\hat{z}. \tag{7}$$

Here the effect of the amplitude gradient is to add an extra term to one component of the fields, proportional to a, phase shifted by $\pi/2$.

The first step is to average the Lagrangian [Eq.(1)] over the gyromotion, which will give the equations for the guiding center. This process should give the same results as the standard procedure of averaging the equations of motion, as it was indeed shown by Littlejohn [4], for the case of static electric and magnetic fields. In the Appendix we derive the guiding center drift velocities from the Lagrangian method, to show that the standard drifts are recovered. Here we use the potentials (2) and (3) to obtain the particle motion in the wave field. Guiding center coordinates are used, as defined in Eqs.(20) and (21) of the Appendix.

2.1. O-Mode

Starting with the O-mode, the averaged Lagrangian is

$$\overline{L_o} = mu_\parallel \dot{z} - mc(c^2+u^2)^{1/2} + \frac{mu_\perp^2\dot{\theta}}{2\Omega} - \frac{e}{c}B_0 X\dot{Y} - \frac{e}{c}\frac{B_1\dot{z}}{a^2+k^2} \times I_0\left(\frac{au_\perp}{\Omega}\right) J_n\left(\frac{ku_\perp}{\Omega}\right)[a\cos(kX+\psi) - k\sin(kX+\psi)]e^{-aX}, \quad (8)$$

where the capital letters refer to the guiding center position, $J_n(x)$ and $I_0(x)$ are Bessel and modified Bessel functions, with $n = \omega/\Omega$, and $\psi = \theta - \omega t$. As a particular, but important case, we consider the resonance condition at the first harmonic $n = 1$, since this is the situation most used in experiments of EC resonance heating at perpendicular injection, because it has the highest absorption. If we approximate for small arguments of the Bessel functions (*i.e.* small gyroradius), $J_1(x) \sim x/2$, $I_0(x) \sim 1$, the Lagrangian becomes

$$\overline{L_o} = mu_\parallel \dot{z} - mc(c^2+u^2)^{1/2} + \frac{mu_\perp^2\dot{\theta}}{2\Omega} - \frac{e}{c}B_0 X\dot{Y} - \frac{e}{c}\frac{B_1\dot{z}}{a^2+k^2}\left(\frac{ku_\perp}{2\Omega}\right) e^{-aX}[a\cos(kX+\psi) - k\sin(kX+\psi)]. \quad (9)$$

From this Lagrangian we can obtain the Euler-Lagrange equations of motion. The equation for the variable $u_\parallel$ gives the condition $\dot{z} = u_\parallel/\gamma$, as expected. The drift velocities are obtained from the equations for X, Y and z, which, when combined, give

$$\dot{X} = 0, \quad (10)$$

$$\dot{Y} = \frac{B_1^2}{B_0}\left(\frac{ku_\perp}{2\Omega}\right)^2 \frac{q}{m\gamma c}\frac{e^{-2aX}}{a^2+k^2}\cos(kX+\psi)\times [a\cos(kX+\psi) - k\sin(kX+\psi)] = -\frac{q(k\rho)^2}{8B_0 m\gamma c}\frac{d}{dX}\overline{A_z}^2, \quad (11)$$

$$\dot{z} = \frac{qB_1}{m\gamma c}\frac{ku_\perp}{2\Omega}\frac{e^{-aX}}{a^2+k^2}[a\cos(kX+\psi) - k\sin(kX+\psi)] = -\frac{q}{m\gamma c}\frac{k\rho}{2}\overline{A_z}, \quad (12)$$

where ρ is the gyroradius. This tells us that there is no drift in the x-direction, and the drift in y is due to a force along the x-axis. This is the ponderomotive force due to the gradient of the fields in the x-direction, which is written here in terms of the gradient of the averaged potential $\overline{A_z}$ squared. In the absence of a background magnetic field, and when the **E**-field variation has a component along its own direction, the PM force is proportional to ∇E^2, but in this case the wave E-field is normal to the gradient, and thus it has no effect on the motion in the plane normal to $\mathbf{B}_0$. Here, the component responsible for the PM force is the wave magnetic field B_1, which in Eq.(11) appears in terms of A_z. We see from Eq.(12) that there is also a drift in z, which is due to the fact that the field E_z felt by the particle changes magnitude as it completes one orbit, and then the positive and negative displacements do not exactly cancel. The drift velocity along $\mathbf{B}_0$ should be given by the time integral of E_z which is A_z, as shown in Eq.(12).

At this point it is possible to mention some aspects of the motion when the resonance condition $n = 1$ is not fulfilled. In that case, one has to use the corresponding Bessel function, which for small argument goes like $J_n(x) \sim (x/2)^n/n!$. Then, when $\omega \ll \Omega$ ($n \ll 1$) this gives a number close to one and therefore Eqs.(11) and (12) are almost the same, but with the factor $k\rho$ replaced by one; the drifts are important. It will be equivalent to the case without a magnetic field since in a wave period the particle behaves like its guiding center. On the other hand, when $\omega \gg \Omega$ ($n \gg 1$) the Bessel function is close to zero, meaning that the drifts become negligible. This is due to the fact that the fast oscillation acts as a random forcing during a gyroperiod., and there is no net effect.

The remaining Euler-Lagrange equations, corresponding to the variables $u_\perp$ and θ, are related to the actual particle gyromotion, giving the perpendicular energy gain and phase evolution. These are important to resonance heating studies [5], but not for our purposes, so we do not give them here. For the X-mode they are coupled to the other equations, so they will be needed as we will show in the following part.

2.2. X-mode

Next we consider the X-mode. This is more complicated since there are more effects involved, like two field components and a gradient parallel to **E**. The averaged Lagrangian is now

$$\overline{L_x} = mu_\parallel \dot{z} - mc(c^2+u^2)^{1/2} + \frac{mu_\perp^2\dot{\theta}}{2\Omega} - \frac{e}{c}B_0 X\dot{Y} + \frac{e}{c}A_1 e^{-aX} J_n\left(\frac{ku_\perp}{\Omega}\right)$$
$$\times\Big\{ I_0\left(\frac{au_\perp}{\Omega}\right)[\dot{X}\cos(kX+\psi) - \xi\dot{Y}\sin(kX+\psi)] + I_1\left(\frac{au_\perp}{\Omega}\right)[\xi\frac{u_\perp\dot{\theta}}{\Omega}\sin(kX+\psi) - \frac{\dot{u}_\perp}{\Omega}\cos(kX+\psi)]\Big\}, \quad (13)$$

where $\xi = A_2/A_1$. In this case, the important situation is for the second harmonic and not the first, since that is where the X-mode is absorbed the most. Then we can take the small argument approximations,

$$J_1(x) \sim x^2/8, \quad I_1(x) \sim x/2$$

and obtain

$$\overline{L_x} = mu_\parallel \dot{z} - mc(c^2+u^2)^{1/2} + \frac{mu_\perp^2\dot{\theta}}{2\Omega} - m\Omega X\dot{Y} + \frac{\Omega_1 u_\perp^2 k}{8\Omega^2}e^{-aX}$$
$$\times\Big\{\Big[\dot{X} - \frac{au_\perp\dot{u}_\perp}{2\Omega}\Big]\cos(kX+\psi) - \xi\Big[\dot{Y} - \frac{au_\perp^2\dot{\theta}}{2\Omega^2}\Big]\sin(kX+\psi)\Big\}, \quad (14)$$

where $\Omega_1 = qkA_1/mc$ is the cyclotron frequency in the wave magnetic field. The Euler-Lagrange equations of this Lagrangian are now coupled, so we have to derive all of them and then solve the system of equations. Only the two equations for $u_\parallel$ and z are decoupled from the others and these give $u_\parallel = \gamma\dot{z} = \text{constant}$ as in the O-mode. The other four equations form the system

$$\begin{aligned} F\dot{Y} - b_1\dot{u}_\perp - c_1\dot{\psi} &= R_1, \\ b_2\dot{u}_\perp + c_2\dot{\psi} + F\dot{X} &= 0, \\ -a_3\dot{Y} + c_3\dot{\psi} + d_3\dot{X} &= R_3, \\ a_4\dot{Y} + b_4\dot{u}_\perp + c_4\dot{\psi} + d_4\dot{X} &= R_4, \end{aligned} \quad (15)$$

where the coefficients are

$$\begin{aligned}
a_3 &= \frac{\Omega_1 k u_\perp}{4\Omega}\xi e^{-aX}\sin\alpha, \qquad a_4 = \frac{\Omega_1 k u_\perp}{8\Omega}\xi\cos\alpha, \\
b_1 &= \frac{u_\perp^3 ka\Omega_1}{16\Omega^5}e^{-aX}\Big[(a - \frac{4\Omega^2}{au_\perp^2})\cos\alpha + k\sin\alpha\Big], \quad b_2 = \frac{u_\perp k\Omega_1}{4\Omega^3}\xi e^{-aX}\sin\alpha, \\
b_4 &= e^{aX} - \frac{\Omega_1 kau_\perp^2}{16\Omega^3}(1-4\xi)\sin\alpha, \qquad c_4 = \frac{ka\Omega_1 u_\perp^3}{32\Omega^3}\xi\cos\alpha, \\
c_1 &= \frac{u_\perp^2 k\Omega_1}{8\Omega^3}e^{-aX}\Big[(1 - \Big(\frac{au_\perp}{2\Omega}\Big)^2\xi)\sin\alpha + \frac{kau_\perp^2}{4\Omega^2}\xi\cos\alpha\Big], \\
c_2 &= \frac{u_\perp^2 k\Omega_1}{8\Omega^3}\xi e^{-aX}\cos\alpha, \qquad c_3 = \frac{u_\perp}{2\Omega}[1 + \frac{ka\Omega_1 u_\perp^2}{8\Omega^3}e^{-aX}(2\xi-1)\sin\alpha], \\
d_3 &= \frac{\Omega_1 k u_\perp}{4\Omega^2}e^{-aX}[(1 - \frac{a^2u_\perp^2}{4\Omega^2})\cos\alpha - \frac{kau_\perp^2}{4\Omega^2}\sin\alpha], \\
d_4 &= \frac{ka\Omega_1 u_\perp^3}{16\Omega^3}\xi[k\cos\alpha - (a - \frac{2\Omega^2}{a\xi u_\perp^2})\sin\alpha], \qquad R_1 = \frac{k^2 a\omega u_\perp^4}{32\Omega^4}\frac{B_{1x}}{B_0}, \\
R_3 &= \frac{u_\perp}{\gamma} - \frac{\omega u_\perp}{2\Omega}[1 + \frac{ka\Omega_1 u_\perp^2}{4\Omega^3}\xi e^{-aX}\sin\alpha], \qquad R_4 = \frac{ka\Omega_1 u_\perp^3}{32\Omega^3}\omega\xi\cos\alpha,
\end{aligned}$$

and the abbreviations $\alpha = kx - \omega t$ and

$$F = 1 + (B_{1x}/B_0)(k^2 u_\perp^2/8\Omega^2)$$

were used. Here, B_{1x} is the full wave magnetic field of Eq.(7). The system (15) can be solved in terms of the determinant of the system matrix which contains terms of different orders in the fields. To first order in Ω_1, it is

$$\Delta = -F^2 b_4 c_3 = -e^{aX}\frac{u_\perp}{2\Omega} - \frac{\Omega_1 k a u_\perp^3}{8\Omega^4} \times[a(\xi - 3/4)\sin\alpha + k\xi\cos\alpha] + O(\Omega_1^2). \quad (16)$$

Then, any of the four variables can be solved for in terms of Δ. We are mainly interested in the drift velocity along y, which is a cumbersome expression, but keeping only terms to second order in Ω_1, which is what we need to get the contribution of the non linear PM force, one has

$$\dot{Y} = \Delta^{-1}e^{aX}\left\{\Omega_1\frac{k u_\perp^3 e^{-aX}}{8\Omega^3}\left(\frac{1}{\gamma} - \frac{\omega}{2\Omega}\right)\sin\alpha + \frac{B_{1x}}{B_0}\frac{k^2 a u_\perp^5}{32\Omega^4\gamma} + \Omega_1^2\frac{k^2 a u_\perp^5 e^{-2aX}}{64\Omega^6} \times\left[\frac{a\xi u_\perp^2}{8\Omega^2}\left(\left(\frac{2\xi\omega}{\Omega} - \frac{4\omega}{\Omega} + \frac{1-4\xi}{\gamma}\right)k\cos\alpha\sin\alpha - \left(\frac{(4\xi+1)\omega}{2\Omega} + \frac{2\xi}{\gamma}\right) \times a\sin^2\alpha + \left(\frac{a}{\gamma} - \frac{4\Omega^2}{a u_\perp^2\gamma} + \frac{4\omega\Omega}{a u_\perp^2} + \frac{2k^2\xi}{a\gamma}\right)\cos^2\alpha + (4\xi - 1)\left(\frac{1}{2\gamma} - \frac{\omega}{4\Omega}\right) \times(k\cos\alpha - a\sin\alpha) - \frac{a\omega}{\Omega}\right) + (4\xi - 1)\left(\frac{1}{4\gamma} - \frac{\omega}{8\Omega}\right)\sin\alpha - \left(\frac{\omega}{2\Omega} + \frac{1}{\gamma}\right) \times\xi\sin^2\alpha + \left(\frac{1}{\gamma} - \frac{\omega}{2\Omega}\right)\frac{k\xi}{a}\cos\alpha\sin\alpha\right] + O(\Omega_1^3)\right\}. \quad (17)$$

This expression includes various effects resulting from the special wave electric and magnetic field properties, including spatial and time dependence and the relativistic contributions. The first two terms are linear in the fields and result from standard linear drifts, while the remaining terms are the result of non linear forces along the x-direction, the PM forces. In this description, they show all the explicit and long dependences, and thus it looks hard to characterize them in terms of a closed expression for the force. A relatively general expression for the PM force in a plasma was derived in [6], which for particles of species α has the form,

$$\mathbf{F}_{p\alpha} = \frac{1}{2}\mathrm{Re}\left\{\frac{i}{\omega}\nabla\mathbf{E}_\omega^*\cdot\mathbf{j}_{\alpha\omega} - \nabla\cdot\left[\mathbf{j}_{\alpha\omega}\left(\frac{i}{\omega}\mathbf{E}_\omega^* + \frac{4\pi\mathbf{j}_{\alpha\omega}^*}{\omega_{p\alpha}^2}\right)\right]\right\}, \quad (18)$$

where the current is

$$\mathbf{j}_{\alpha\omega} = n_\alpha q_\alpha^2\mathbf{E}/m_\alpha\omega,$$

and

$$\omega_{p\alpha}^2 = 4\pi n q_j^2/m_j.$$

The effect of time dependence of the PM force is not included there. The contribution of the wave magnetic field is not apparent in Eq.(18) because it was eliminated using Faraday's law, but it does contribute too. One can use expression (18) with the fields we are considering, given by Eq.(6) and find an expression consistent with Eq.(17), with small differences due to the aforementioned neglect of the time dependence. Therefore, we can conclude that the second order terms in Eq.(17) are the result of a PM force, as we would have expected.

The remaining expressions for $\dot{X}$, $\dot{u}_\perp$ and $\dot{\psi}$ are equally involved as Eq.(17), but since they are not relevant for our discussion, we do not give them here.

3. Numerical computation of trajectories

In the previous section we found analytical expressions for the particle drifts, which turned out to be quite complicated, but it was possible to single out the presence of the PM force in the second order terms. However, although the averaged Lagrangians (8) and (13) were derived for arbitrary wave frequency, the results for the particle drifts were obtained for the particular resonant cases: $\omega = \Omega$ (O-mode), $\omega = 2\Omega$ (X-mode), which are the most common situations in the experiments. A general expression for the drift, including off-resonance cases, would be extremely involved making its analysis practically impossible. Instead, in this section we are going to compute the detailed particle orbits by numerically solving the equation of motion in the corresponding electromagnetic fields. In this way it will be possible, not

only to compare resonant and off-resonance cases, but also to look at the orbit differences between O- and X-modes.

The equation of motion to solve is

$$m\frac{d\mathbf{u}}{dt} = q[\mathbf{E}_w + \frac{1}{c}\mathbf{u}\times(B_0\hat{z} + \mathbf{B}_w)], \qquad (19)$$

where the wave fields $\mathbf{E}_w$, $\mathbf{B}_w$ are those given by Eqs.(4)-(7) for each mode. We use a Runge-Kutta method to obtain both the particle orbit and the velocity. We consider the motion in a standing wave, so the spatial dependence in the argument in the sinusoidal functions is not included. This is done to simplify the shape of the orbits and it is appropriate for a particle near a resonance where the wave is being absorbed. In the following, the orbits are represented by its projection on the $x-y$ plane, since we are not interested in the parallel motion. As one may expect, there are many different possible orbits depending on the field and particle parameters and their relative phases. We will show a few representative cases to visualize the relevant points.

3.1. O-mode

We first consider a case with the resonance condition $w = \omega/\Omega = 1$ for a high intensity wave in which the wave field amplitude is 50% of the background magnetic field. The particle trajectory depends on the relative phase with the wave, *i.e.* the parameter θ used in Sec. 2. For this resonant case, the process of energy absorption by the particles takes place in a statistical way, as it has been discussed by Taylor *et al.* [5]. As they have shown, the wave produces an energy redistribution of particles over a closed contour in the energy-θ space, so that, the particles, that are initially in the low energy side of the contour have an average energy gain. Since we are not interested here in the process of energy absorption, we will consider a single phase which may or may not show an energy gain. In Fig. 1 we show the comparison of the orbits and the velocity vectors of a positive particle, for cases with ($a = 0$) and without ($a \neq 0$) a field gradient. The magnetic field points outwards and the wave comes from the left. For the case with a gradient, the wave amplitude is constant for $x < 0$ and it has the exponential drop, e^{-ax} for $x > 0$, with a equal to the particle gyroradius. So, the wave starts being absorbed at $x = 0$. It is seen that, for this phase, the projection of the orbit in the case with no gradient is complicated, but there is no mean displacement; that is, the orbit stays bounded. We note, in passing, that the apparent gyroradius changes do not necessarily mean a change in energy, since the orbit is just a projection in the $x-y$ plane. In contrast, with the exponential gradient one can see that there is a drift motion in the direction of $-y$. The drift is the result of the $x-$dependence of the wave amplitude, giving a PM force $\mathbf{F}_p$ in the x direction, and a $\mathbf{F}_p\times\mathbf{B}$ drift velocity. In this particular case, there is also a concurrent particle energy gain, as seen in the gyroradius and velocity magnitude continuous increase. For all other initial phases the characteristic feature of the y-drift is always present, but not the radius increase.

A case away from a resonance is shown in Fig. 2, with $w = 1.5$. The other parameters are the same as those in Fig. 1. Here it is seen that the orbit without gradient remains bounded as in the resonant case, whereas the trajectory in presence of a gradient shows a displacement along the direction $-y$, but it is apparent only after several orbits. It is interesting to note that the shape of orbits is not sensitive to the relative phase of the wave and particle gyromotion, which would be expected for a non resonant interaction. Finally, in Fig. 3, we show the orbits for a wave resonant at the second harmonic: $w = 2$, the other parameters kept equal.

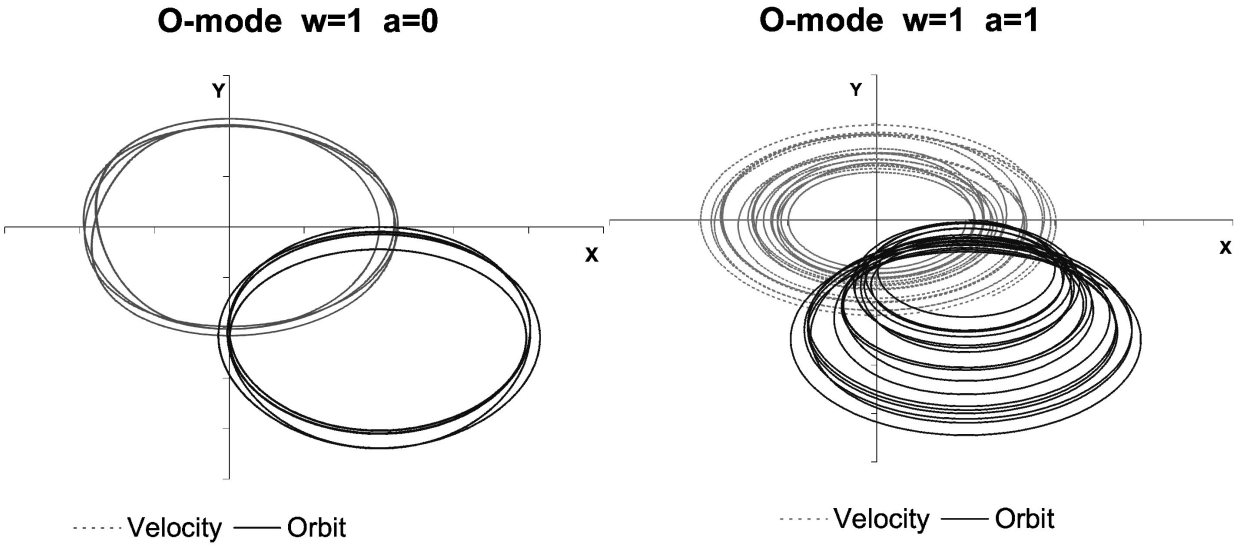

FIGURE 1 Particle orbit and velocity vector in a constant background magnetic field $\mathbf{B}_0 = B_0\hat{z}$ and an electromagnetic wave with the electric vector parallel to $\mathbf{B}_0$ (O-mode). On the left is the case with constant wave amplitude, and the right plot is for an amplitude varying as e^{-ax} with $a = 1$, in the region $x > 0$. The wave is in resonance with the gyromotion, $w = \omega/\Omega = 1$, and has amplitude 50% B_0 at $x = 0$.

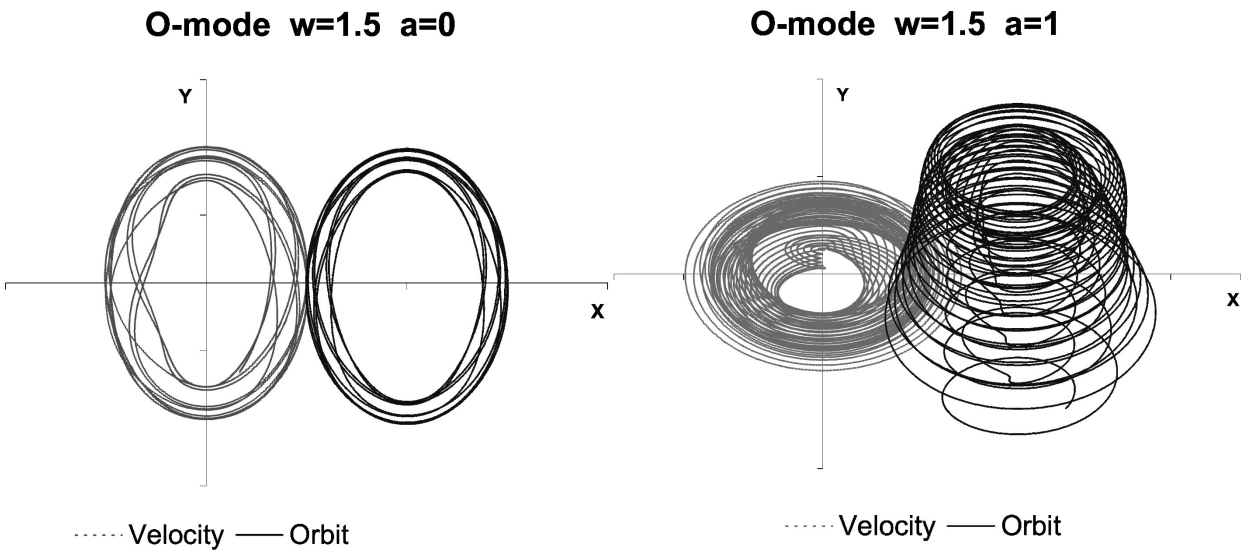

FIGURE 2 The same as in Figure 1 but for the non resonant situation $w = 1.5$.

The orbits are similar to the case of the fundamental resonance in that they depend strongly on the initial phase, and the drift in y is only present when the wave amplitude gradient in included. We notice that the drifting motion is not always steady, but it has periods of up and down motion, although, on average, the guiding center moves downwards. It is appropriate to point out that, part of the difference between the cases $a = 0$ and $a = 1$ is due to the fact that the E-field has an additional term proportional to $\sin\theta$, when $a = 1$ as it is seen in Eq.(4). A general result is that, in all cases, wave absorption causes the particle to drift in the same direction.

3.2. X-mode

Next we turn to the more complicated case where the electric field is normal to $\mathbf{B}_0$. Here, the two components of the electric field give rise to drifts even in the absence of field gradients, which is reflected in the first order terms of Eq.(17). The parameters used in the computations are the same as in the O-mode. Due to the presence of the drifting motion, even in the absence of a gradient, the orbits cannot be drawn for times as long as in the O-mode, so only a few cycles are shown. The case with $\omega = \Omega$ is depicted in Fig. 4, comparing the situations without and with absorption. One can see that for $a = 0$ the drift is in the direction of $-y$, which is the same as the direction of the drift expected from the PM force. For this reason, in the orbit for $a = 1$ there is no qualitative difference with the orbit without absorption, except that there is an additional drift along the negative x-axis, coming from the E_y component that interacts with the additional term of B_z proportional to a [see Eq.(7)], but it has no relation with the PM force.

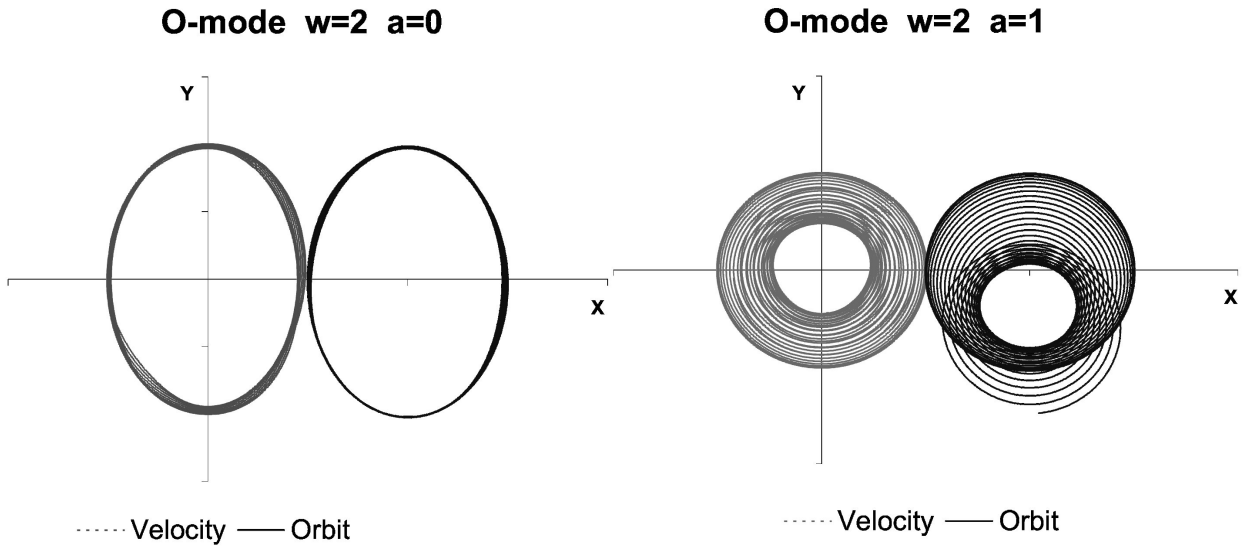

FIGURE 3 Particle orbits and velocities for a wave resonant at the second harmonic $w = 2$, with the same conditions of Figure 1.

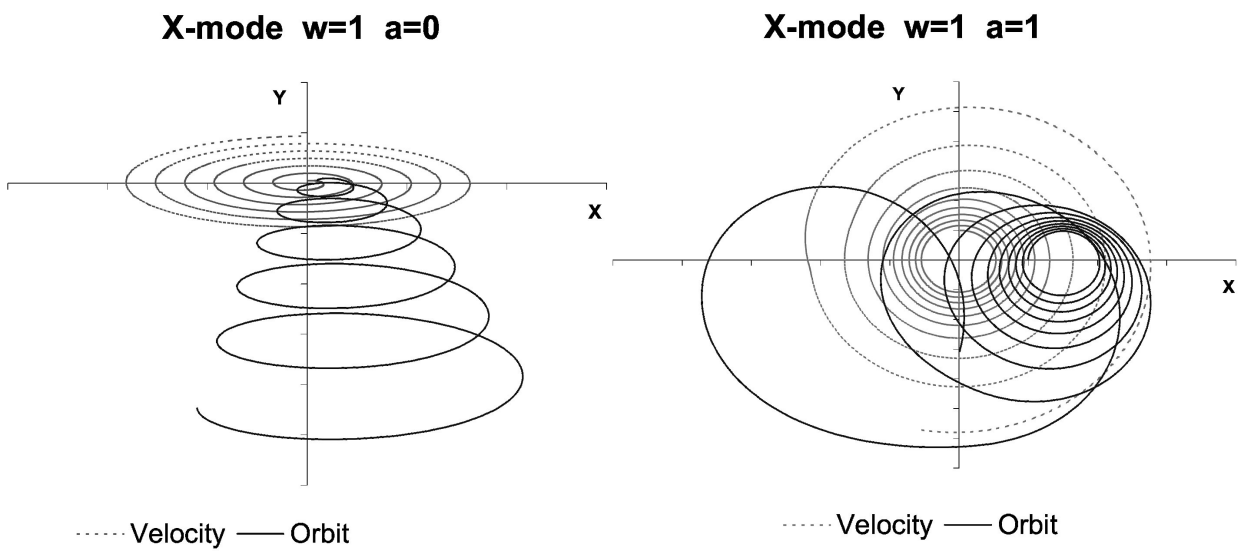

FIGURE 4 Particle orbits and velocity vectors for motion in a constant magnetic field along the z-axis and an electromagnetic wave with the electric vector in the plane $x-y$ (X-mode). The wave amplitude varies as e^{-ax} and it is constant for $x<0$, with a magnitude of 40% B_0. The left plot corresponds to a constant amplitude ($a=0$). The wave has the fundamental resonant frequency: $w=1$.

The presence of the PM force can only be inferred from the slight differences in the y-drifts. In contrast, the cases for out-of-resonance ($w=1.5$) and for the second harmonic ($w=2$), shown in Figs. 4 and 5, respectively, have a drift in the direction x, when $a=0$. Therefore, the contribution from the PM force when $a=1$ is quite clear, since it changes the drift to the $-y$ direction, in both cases (the wave amplitude was a little weaker than before: 40% of B_0). The reason for the difference between the cases with $w=1$ and $w=1.5,2$ for no wave absorption is that, of the two E-field components, E_x is the one that interacts more strongly with the particle at the fundamental resonance, but for all other cases E_y is the most efficient component.

An interesting behavior that is noticed from the figures is that, when absorption is included the particle energy is continuously increased, even for $w=1.5$, as it can be told from the increase in the velocity magnitude. Note that, in contrast to the O-mode, now there is no motion along $\mathbf{B}_0$ since $\mathbf{E}$ is normal to it, so the velocity in the $x-y$ plane is the total velocity. It then results that, while for $a=0$ there is no energy transfer for frequencies different from the main resonance, the presence of a gradient amplitude allows for energy absorption. This is due the additional term in the B-field proportional to $a\sin\theta$, in Eq.(7), that contributes only for $a\neq 0$.

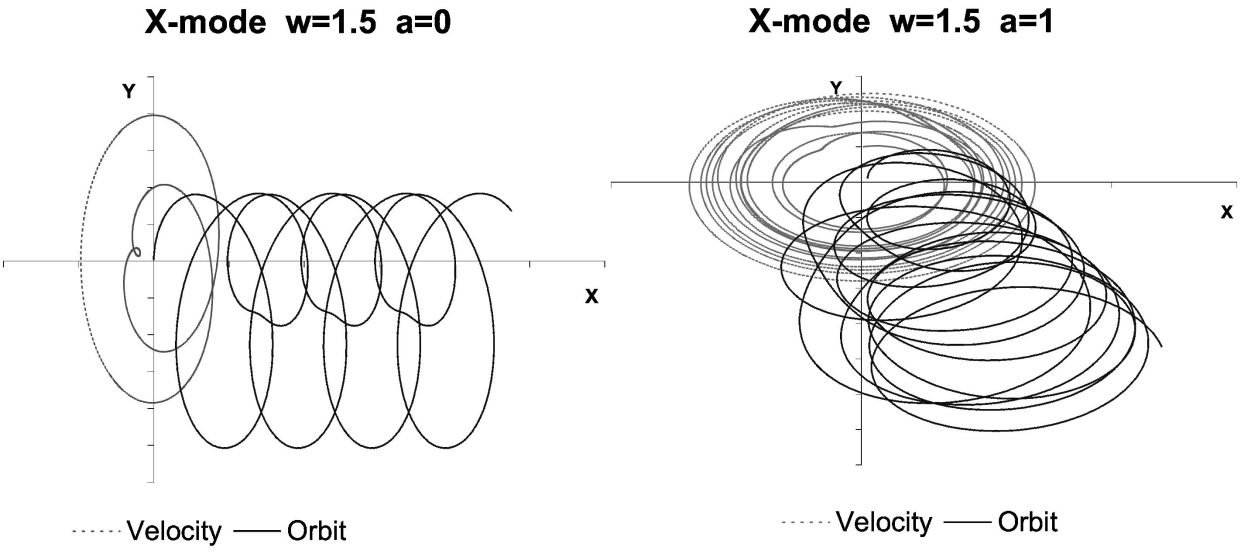

FIGURE 5 Same situation as that of Figure 4 but for a non resonant wave with $w=1.5$.

This phase-shifted contribution interacts constructively with the field E_y. Another worth-noting feature that is apparent from the orbits presented is that, in some cases the guiding center drift does not necessarily involve a net displacement of the particle, since it is associated with a simultaneous gyroradius increase. This happens for both the O-mode and the X-mode. Thus, it would be possible to have a mean particle flux, represented by the guiding centers flow, with the particles still crossing through a fixed point.

4. Conclusions

It has been shown that the particle motion in a magnetized plasma when an electromagnetic wave is injected and absorbed, reflects the presence of a ponderomotive force due to the wave amplitude spatial decrease. The effect is manifest by a $\mathbf{F}_p \times \mathbf{B}_0$ drift velocity of the guiding center. This result was obtained both by an analytical procedure based on a Lagrangian description and by a numerical solution of the trajectories. The two wave polarizations (O-mode and X-mode) were considered. The O-mode is simpler to study because the wave electric field is parallel to $\mathbf{B}_0$ and plays a minor role. For this case, a closed analytical expression for the drift velocity was obtained [Eq.(11] for the fundamental resonance ($\omega = \Omega$) which qualitatively coincided with the numerical results for the orbits. In the case of the X-mode, we did not find a complete analytical expression, which would include terms up to fourth order in the wave amplitude, but found an approximation to second order. That formula shows the effect of the non linear PM force. As before, the numerical results agreed qualitatively with the prediction of Eq.(17) for the case of the second harmonic resonance ($\omega = 2\Omega$). The numerical studies, which can be made for a wider range of conditions than the analytical ones, have indicated that the effect of the PM force is important for all wave frequencies. We used very high wave amplitudes in order to make the nonlinear effects more evident: an amplitude of half the value of B_0, for the magnetic fields used in tokamaks, corresponds to a power density of $10GW/cm^2$. More realistic wave powers will produce the same effect but over a larger time, that is, after more gyro-orbits. The drifting motion of the guiding center can be quite irregular, with periods of direction inversion and, for resonant frequencies, it does not always involve particle displacement. This latter situation arises because the gyroradius increases while the particle is drifting (*e.g.* Figs. 4 and 6), but nevertheless, there is an average particle flux.

The confirmation that the absorption of an electromagnetic wave at the resonant surface of a plasma produces a particle flux in a direction perpendicular to $\mathbf{B}_0$ and the wave gradient (which is usually the direction of propagation), is an important result since the flux can have relevant effects on plasma dynamics. A particularly interesting consequence of this flux is the possibility of driving plasma rotation near the edge of a tokamak plasma, proposed in Ref. 2. That mechanism is based on the injection of high-power EC waves in the radial direction, so that the absorption scale a is of the order of the electron gyroradius, and thus the field gradient is high enough to produce a significant particle flux in the poloidal direction. The flux is poloidally asymmetric and if there are enough collisions the friction force $\mathbf{f}$, produces a radial flow by the $\mathbf{f} \times \mathbf{B}$ drift, which has the same asymmetry. Under this conditions, the plasma can start rotating due to the spin-up mechanism proposed by Stringer [8].

Acknowledgments

This work was partially supported by research projects 27974-E from Conacyt and IN116200 from DGAPA-UNAM, MEXICO.

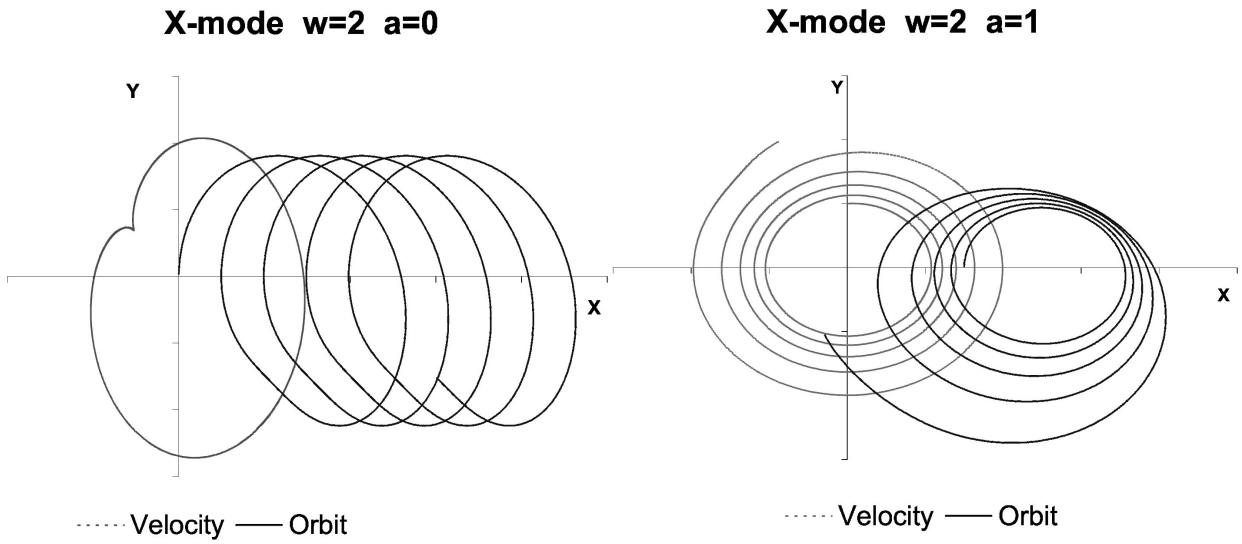

FIGURE 6 Same situation as that of Figure 4 but for resonance at the second harmonic: $w = 2$.

A Appendix: Particle drifts with the Lagrangian method.

The orbit theory of charged particles in electromagnetic fields is well known. The particle motion in presence of a magnetic field is usually described with the guiding-center approximation, which separates the gyromotion, represented by $\mathbf{u}$, from the displacement of the guiding center, or drift velocity $\mathbf{w}$, resulting from the action of all the agents additional to the constant and uniform magnetic field $\mathbf{B}$ [7]. The total particle velocity is $\mathbf{v} = \mathbf{w} + \mathbf{u}$. Thus, one has for instance the electric drift, $\mathbf{w}_E = c\mathbf{E} \times \mathbf{B}/B^2$, when there is a constant and uniform E-field, the curvature and grad-B drift,

$$\mathbf{w}_B = (mc/qB^4)(v_\parallel^2 + v_\perp^2/2)[\mathbf{B} \times \nabla(B^2/2)],$$

or the polarization drift,

$$\mathbf{w}_p = (m/qB^2)d\mathbf{E}/dt,$$

when the electric field is time dependent. It should be recalled that the guiding-center description is useful only when the space and time variations of the fields are small compared to the particle gyroradius and gyroperiod, respectively. When the background B-field does not satisfy these conditions, particle trajectories must be obtained directly by solving the equations of motion. On the other hand, when there is an oscillatory electric field, a description similar to the guiding center is possible, separating the motion of the center of oscillation and the oscillations about it. In this oscillating-center description, if the electric field varying with frequency ω has a spatial gradient, the oscillating center is subjected to a net force that accelerates it; the so called ponderomotive force:

$$\mathbf{F}_p = -(q^2/2m\omega^2)\nabla E^2.$$

We will show here that the results of the guiding center theory can be obtained from a Lagrangian description., as described in Sec. 2. For a uniform B field in the z-direction, the relevant vector potential is $\mathbf{A} = B_0 x\hat{y}$. In order to allow space and time variations, we will use the more general potential $\mathbf{A} = A_0(t)f(x)\hat{y}$. For completeness, we can also consider an electric potential given by $\phi = \phi_0(t)g(y)$. The corresponding electric and magnetic fields are

$$\mathbf{E} = -[f(x)\dot{A}_0/c + \phi_0 g'(y)]\hat{y},$$

$$\mathbf{B} = A_0 f'(x)\hat{z}$$

(prime denotes space derivatives and over dot denotes time derivatives). Now, we go to guiding-center coordinates, defined by [5]

$$\mathbf{q} = \mathbf{X} + \frac{u_\perp}{\Omega}\sin\theta\hat{x} - \frac{u_\perp}{\Omega}\cos\theta\hat{y}, \qquad (20)$$

$$\mathbf{u} = u_\perp\cos\theta\hat{x} + u_\perp\sin\theta\hat{y} + u_\parallel\hat{z}, \qquad (21)$$

where θ is the gyrophase (Ωt). As mentioned before, the time derivative of $\mathbf{q}$ is no taken to be the same as $\mathbf{v}$, so we have to get it directly from eq.(20). The variations of the fields have to be such that the time variations are slower than the particle gyroperiod, Ω^{-1}, and the space variations are less than the Larmor radius $u_\perp/\Omega$. The Lagrangian is then averaged over a gyroperiod:

$$\overline{L} = \langle [mu_\perp(\cos\theta\hat{x} + \sin\theta\hat{y}) + mu_\parallel\hat{z} - qA_0(t)f(x)\hat{y}] \cdot [\dot{\mathbf{X}} + \frac{\dot{u}_\perp}{\Omega}\sin\theta\hat{x} + \frac{u_\perp\dot{\theta}}{\Omega}\cos\theta\hat{x} - \frac{\dot{u}_\perp}{\Omega}\cos\theta\hat{y} + \frac{u_\perp\dot{\theta}}{\Omega}\sin\theta\hat{y}] - mc(c^2 + u_\perp^2 + u_\parallel^2)^{1/2}\rangle, \qquad (22)$$

where $\langle\xi\rangle = (\Omega/2\pi)\int_0^{2\pi/\Omega}\xi dt$. The result is

$$\overline{L} = mu_\parallel\dot{Z} + mu_\perp^2\frac{\dot{\theta}}{\Omega} - mc(c^2 + u^2)^{1/2} + L_A, \qquad (23)$$

where L_A is the field contribution. This can be expressed in terms of Taylor expansion of the functions $f(x), g(y)$ etc. about the guiding center, up to second order, as

$$L_A = q\phi_0[g(Y) + g''(Y)\frac{r_L^2}{4}] - \frac{q}{c}A_0[f(X) + f''(X)\frac{r_L^2}{4}]\dot{Y}, \qquad (24)$$

where $r_L = u_\perp/\Omega$ is the Larmor radius. Then, the relevant variables are $z_i = (X, Y, Z, u_\parallel, u_\perp, \theta)$. The Euler-Lagrange (EL) equations will give the guiding-center motion and gyromotion. The particle drifts are obtained from the EL equations for $\mathbf{X}$.

By taking the EL equation for Y, it is easy to see that when the space variations are ignored, one obtains the $\mathbf{E}\times\mathbf{B}$-drift

$$\dot{X} = -\frac{f(x)\dot{A}_0 + c\phi_0 g'(y)}{A_0 f'(X)} = c\frac{E}{B}. \qquad (25)$$

If the space dependence is kept, finite-Larmor-radius corrections arise in the previous drift, and the grad-B drift results, when the EL equation for X is derived:

$$\dot{X} = -\frac{c\phi_0(g'(Y) + g'''(Y)r_L^2/4) + \dot{A}_0(f(X) + f''(X)r_L^2/4)}{A_0(f'(X) + f'''(X)r_L^2/4)}, \tag{26}$$

$$\dot{Y} = -\frac{A_0 f''(X)\dot{\theta}r_L^2/4}{A_0(f'(X) + f'''(X)r_L^2/4)} = -\frac{u_\perp^2}{2\gamma\Omega}\frac{B'}{B}, \tag{27}$$

where the B-field also contains finite-Larmor-radius corrections. These expressions agree with the standard results [7].

1. G.G. Craddock and P.H. Diamond, *Phys. Rev. Lett.* **67** (1991) 1535.
2. J.J. Martinell and C. Gutiérrez-Tapia, *Phys. Plasmas* **8** (2001) 2808.
3. R. Klima, *Czech. J. Phys. B* **18** (1968) 1280.
4. R.G. Littlejohn, *J. Plasma Phys.* **29** (1983) 111.
5. A.W. Taylor, R.A. Cairns and M.R. O'Brien, *Plasma Phys. Controlled Fusion* **30** (1988) 1039.
6. R. Klima, *Czech. J. Phys. B* **30** (1980) 874.
7. T.G. Northrop, *The adiabatic motion of charged particles*, (John Wiley & Sons, New York 1963).
8. A. Hassam and J. Drake, *Phys. Fluids B* **5** (1993) 4022.